

Vehicle Impact Response Analysis Through the Use Of Accelerometer Data

Michael S. Varat and Stein E. Husher
KEVA Engineering

Copyright © 2000 Society of Automotive Engineers, inc.

ABSTRACT

Staged collision test data includes instrumentation in order to measure acceleration time histories, force time histories and other engineering parameters. The output from these instruments allows the analysis of vehicle energy absorption and collision pulse shape characteristics. Additionally, crash test repeatability, velocity sensitivity, and the influence of rigid versus deformable barriers may be investigated.

The present study analyzes collision pulse shapes including analytical relationships and pulse parameters. Closed form functions are applied and compared to the observed experimental pulse shapes. Differences between analytical predictions and observed experimental results are explored. Techniques are presented whereby collision pulses can be analyzed and applied to the reconstruction of real world automobile collisions. The use of acceleration time histories and crash test data in the determination of vehicle structural characteristics is investigated. Extrapolated force time histories are determined from the measured accelerometer outputs and this data is compared to barrier load cell data. An analysis is then performed to address the appropriateness of using accelerometer data to extrapolate force versus deflection characteristics. Force versus deflection data is determined for the same vehicle type at differing crash test speeds in order to investigate the rate sensitivity of vehicle crush response. The absorbed energy versus vehicle crush is determined from the instrumented crash test data and analyzed for structural impact trends. The analytical determination of static crush, dynamic crush and vehicle structural restitution is investigated.

INTRODUCTION

The engineering analysis and reconstruction of vehicle structural performance and occupant dynamics in real world impacts requires detailed information on forces and accelerations. To accomplish this, a time dependant analysis of the acceleration, vehicle absorbed energy as well as the impact configuration is often used to identify the dynamics. While staged reconstruction collision tests may be performed to duplicate the collision pulse, this approach is not practical under all

circumstances. Therefore, the development of mathematical models to represent the acceleration pulse of a collision is performed.

Collision pulse characteristics generally consist of shape, amplitude and duration. Numerous methods of closed form curve fitting have been applied to collision pulses with varying success. Observed trends have demonstrated that collision pulse characteristics vary based on impact mode, collision partner, and vehicle specific parameters. Previous researchers have applied various functions from simple step to complex trigonometric. Current research indicates that vehicle structural engagement serves as the first factor that influences acceleration response and that collision mode may serve as a useful determinant for collision pulse modeling.

Staged collision test data includes acceleration time histories, force time histories, residual crush, and impacting speed as some of the measured parameters. Tests are conducted at various impact velocities into both rigid and deformable structures. When applying this data to a real world collision event, considerations include rate sensitivity of the vehicle crush, force deflection characteristics, and the appropriateness of the applied force deflection model. These considerations have not all been thoroughly investigated in the literature.

ACCELEROMETER LOCATION

Care must be exercised in the analysis of accelerometer data to ensure that the instrumentation output accurately represents the vehicle under study. Varying locations within the vehicle may have unique kinematic time histories. A significant factor for rigidly mounted accelerometers is whether the instrument is mounted in or out of the crush zone. This factor should be considered when analyzing accelerometer data.

Figure 1 is the accelerometer output for a 35 mph frontal barrier collision test involving a 1982 Chevrolet Citation. The time histories from four accelerometers are shown overlaid. These accelerometers are located on the floorpan at the left front, right front, left rear and right

rear. The trends indicated on the graphs show little variance between the four mounting locations. While small differences are seen in peak accelerations, the overall response shows little variance between the four mounting locations. The only significant difference in acceleration response is seen with the left front accelerometer which shows *some* distinctive differences between 60 and 95 msec due to what may be local buckling of that area of the floorpan late in the collision pulse.

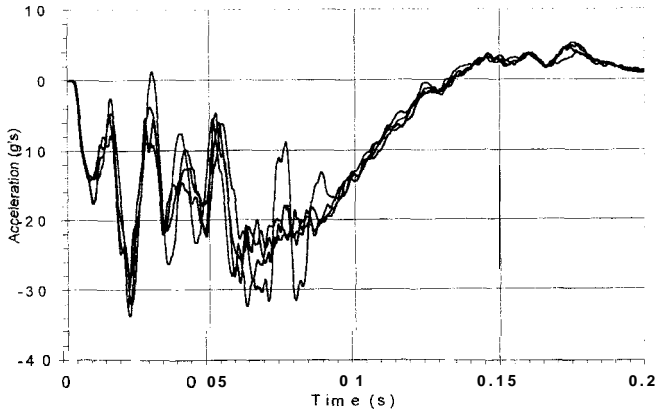


Figure 1. Acceleration pulses at different floorpan mounting locations – 1982 Chevrolet Citation.

In order to demonstrate the large differences that may be seen with different accelerometer mounting locations, consider the extreme case of accelerometer mounting on non-rigid structures within the vehicle. Figure 2 shows the acceleration response for a frontal rigid barrier collision of a 1998 Toyota Camry. The lighter lines on Figure 2 are the accelerometer output from 3 floorpan accelerometers. As can be seen, the floorpan response is fairly constant with little difference seen in the response from the three different instruments.

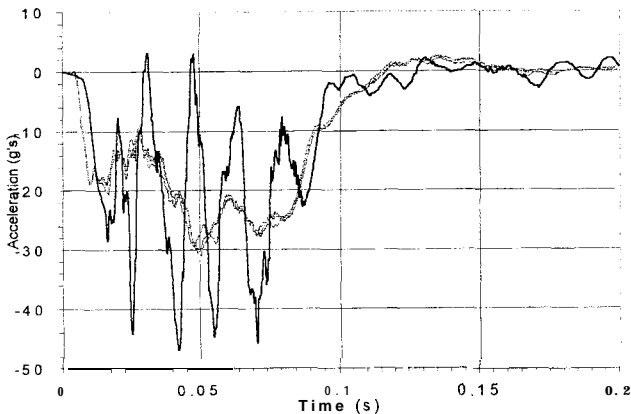


Figure 2. Dash versus floorpan acceleration pulses – 1998 Toyota Camry.

However, when the dash panel accelerometer (darker line) is overlaid onto this graph, significant differences are seen. A vibratory response is seen throughout the collision pulse as the dash panel appears to vibrate around the underlying vehicle floorpan response. If the response for an occupant seated in a normally seated position is desired, clearly the dash panel response shown would be inappropriate to use. Therefore, care must be exercised when using accelerometer data to

ensure that local deformations or vibrations are not affecting the data. This can be seen through carefully examining all available accelerometer data to understand the vehicle impact response.

REPEATABILITY

To address concerns about Anthropomorphic Test Device (ATD) response developed through the New Car Assessment Program (NCAP), the NHTSA initiated the Repeatability Test Program (RTP) [Machey 1984] to study the ATD response variation during frontal barrier crashes of similar vehicles under the similar test conditions. The RTP was conducted using 14 identically equipped Chevrolet Citations manufactured on the same assembly line and on the same shift. These vehicles were then shipped to 3 different NHTSA certified contractors to be tested using the same procedure. The test parameters of interest included impact speeds of 35 +/- 0.5 mph and a target weight of 3000 pounds. Although primarily a dummy response study the accelerometer data from these tests allows the investigation of vehicle response variability under impact conditions. Figure 3 shows the accelerometer output from tests at the same facility. These three Citations were all impact tested at the same target weight and impact velocity. As can be seen, little variability is present between the responses of these three identical vehicles under impact conditions.

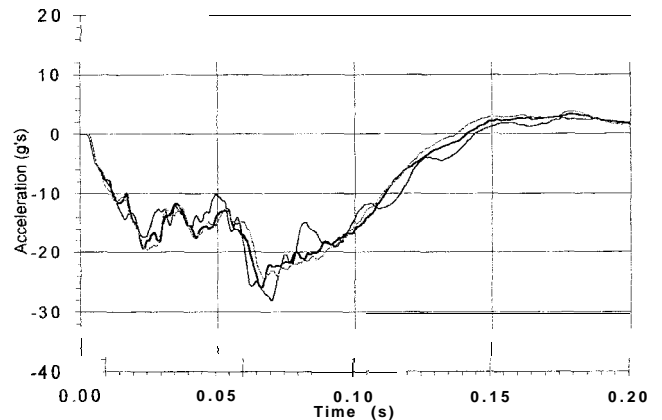


Figure 3. Acceleration pulses of different 1982 Chevrolet Citations at the same test facility.

When examining test variability, the influence of test facility procedures can also be examined. Figure 4 shows the accelerometer output for three identical Citations impact tested by three different facilities. As with Figure 3, it can be seen that little variability exists between these curves. In fact, integration of these curves yields almost identical values for dynamic crush which indicates that test variability may be well controlled for through careful test methodology. It is interesting to note that even though the accelerometer outputs are quite similar, the reported static crush varies as much as 2% inches among vehicles tested in the RTP. This difference in reported static crush leads to the conclusion that the variability is not due to actual test response variability but rather is due to post test static

crush measurement differences. This conclusion agrees with that found in earlier research [Varat, 1994].

--TN 552 TRC --TN 492 Calspan --TN 483 Dynamic Science

$$EAF = \sqrt{\frac{2 \cdot (\text{Crush Energy})}{\text{characteristic width}}}$$

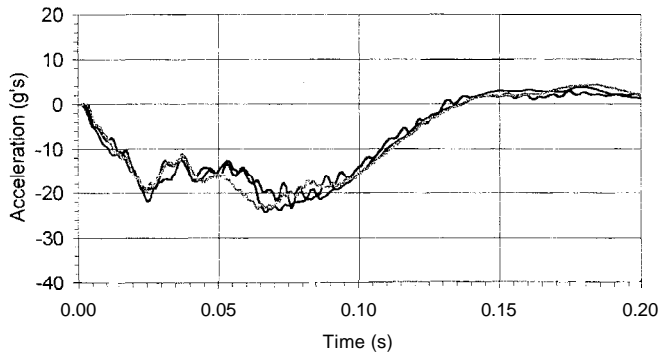


Figure 4. Acceleration pulses of different 1982 Chevrolet Citations at the different test facilities.

COMPARISON BETWEEN LOAD CELL AND ACCELEROMETER INSTRUMENTATION

A control volume energy analysis is used to analyze the energy absorption characteristics of a vehicle. For a frontal, fixed, rigid barrier collision, this analysis is performed by first considering that all of the available energy coming into the collision consists of kinetic energy from the vehicle motion. The vehicle then comes to a stop and rebounds rearward at a velocity dependant on restitution properties. The absorbed energy is then determined as the difference in the pre impact and post impact kinetic energy.

In order to determine the energy absorption characteristics, the derivation of the force deflection relationship is desired. This relationship may be determined from accelerometer data with the assumption of a single mass representing the vehicle body and a massless spring representing the crush zone. Obviously, the crush zone of the vehicle has mass so the validity of this assumption must be further investigated. Then, using Newton’s second law, the acceleration time history may be extrapolated to a force time history through multiplying the mass times the acceleration. The acceleration time history is then integrated twice to arrive at the displacement time history. Lastly the derived force is plotted versus displacement.

A second method of determining the force displacement relationship is to use a direct measurement of force from a load cell barrier and plotting this data versus the displacement determined from a double integration of the accelerometer data.

In order to derive the energy versus displacement, the force-displacement is integrated. This yields the energy versus displacement relationship for the vehicle structure under study. In order to analyze the energy absorption characteristics, an energy factor, EAF is used where EAF has been previously described [Kerkhoff, 1993].

Figure 5 is an acceleration time history for a 1980 Chevrolet Citation undergoing a frontal rigid barrier impact. This collision test yields both acceleration time history as well as barrier load cell data and allows the two to be compared. If the previously described data analysis is performed, Figure 6 is generated and shows the force deflection relationship for the Citation based on two different methods. The dark line shows the force deflection curve based on accelerometer data and the lighter line shows the same curve based on the barrier load cell data. As can be observed, the barrier load cell data appears significantly higher, especially in the area encompassing 8 to 18 inches of crush. At higher deflections, the two curves exhibit less differences.

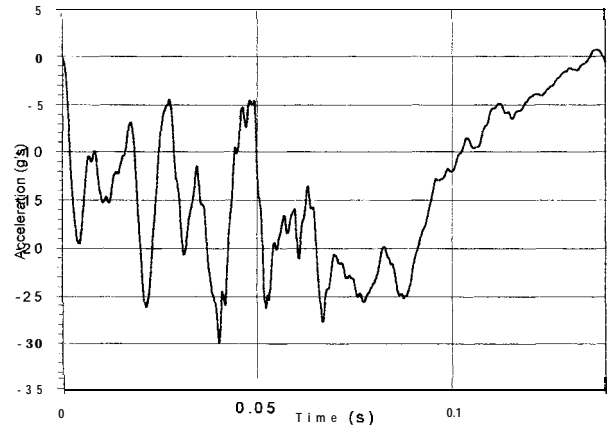


Figure 5. Acceleration pulse – 1980 Chevrolet Citation

In order to investigate the significance of the observed differences in forces seen in Figure 6, the absorbed energy data is examined. Figure 7 is EAF versus crush derived from the two different force deflection curves in Figure 6. Figure 7 demonstrates a marked difference between the load cell and accelerometer derived EAF values. Note that the load cell derived EAF value at maximum displacement is approximately 12% higher than the accelerometer derived EAF.

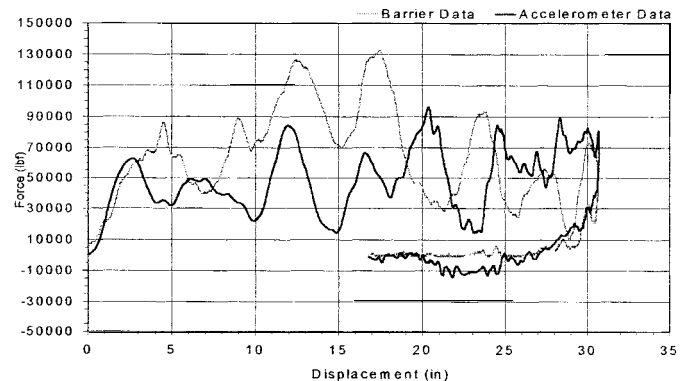


Figure 6. Comparison of force deflection derived from accelerometer versus load cell data.

It has been proposed that the use of accelerometer derived force is not valid due to the mass of the vehicle within the crush zone. The vehicle does not consist of a single mass with a massless spring striking the barrier. Rather, the crush zone (spring area) of a vehicle has mass that may need to be accounted for during the collision sequence. If this hypothesis was true, then any accelerometer derived forces would be too high when compared to the load cell data. However, examination of Figure 7 indicates that the opposite is true. The load cell derived EAF values are higher than the accelerometer derived EAF.

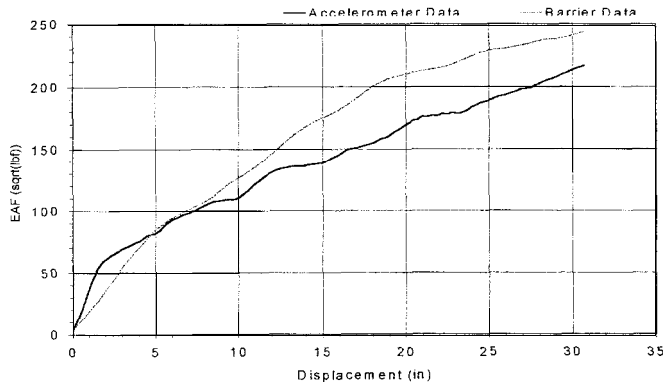


Figure 7. Comparison of EAF versus deflection derived from accelerometer versus load cell data.

Absorbed energy can never exceed the available input energy into the collision event. If one neglects energy sources such as heat, light, sound, then the maximum absorbed energy (assuming zero restitution) is the input kinetic energy ($E = \frac{1}{2} * M * V^2$). If this calculation is performed for the test in Figure 7, it is found that this equates to the maximum EAF seen in the accelerometer derived data. If one examines the load cell derived EAF, it is found that the load cell data equates to an energy higher than the input kinetic energy. Therefore, the load cell derived EAF values are too high. Crash test data sources were examined for numerous test vehicles of varying type and this trend has been observed often whereby the load cell derived energy is too high. This indicates a potential problem with the load cell data. This may be due to bending loads induced due to the area of the load cell plates, unaccounted for inertial effects or other unexamined sources. Additionally, since the accelerometer derived energy matches the input kinetic energy at maximum crush, the proposed mass conservation problems appear to be insignificant for this and other tests examined by the authors.

STRUCTURAL RESPONSE

Accelerometer or load cell generated data enables the analysis of structural response which includes rate sensitivity and restitution properties. Rate sensitivity has been observed for metal structures under applied loads. In order to investigate the rate sensitivity of vehicle frontal structures, consider the following analysis.

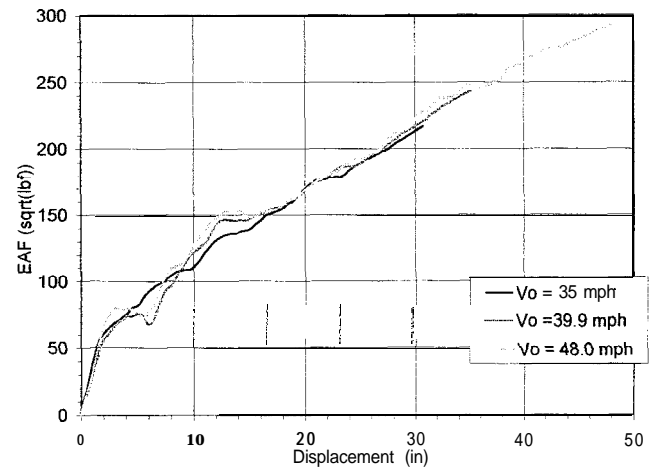


Figure 8. Comparison of EAF versus deflection derived from Citation tests at different velocities.

The Chevrolet Citation tests in Figure 8 were conducted at 35, 40 and 48 mph. It is apparent that there is good correlation with little variance in energy absorption trends with increasing velocity. It is also interesting to note, in Figure 8, that EAF is nearly linear with crush; this indicates a constant stiffness over increasing crush depth after the first two inches of crush.

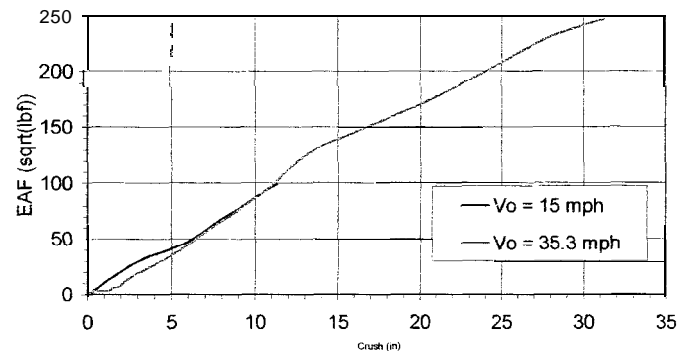


Figure 9. Comparison of EAF versus deflection derived from tests at different velocities.

To further explore velocity dependence, consider the EAF versus crush graph of the Chevrolet S-10 pickup in Figure 9. The first test was at 15 mph and the second test was conducted at 35 mph. As can be seen in Figure 9, similar response is seen between the two test severities, except for the highly elastic region at less than 4 inches crush. **The energy absorption characteristics of the front of the S-10 does not appear to vary with impact velocity. Rather, the energy absorption appears to only be a function of crush depth when the same structures are engaged.** As with the Citation in Figure 8, **the S-10 in Figure 9 also exhibits a linear relationship between EAF and crush.**

RESTITUTION CHARACTERISTICS

Both the acceleration time history and the force time histories are determined as a function of the vehicle dynamic deflection. However, vehicles have restitution

properties such that there is partial elastic rebound of the structure. In order to investigate restitution characteristics, consider a frontal barrier crash test of a 1988 Toyota Camry. Figure 10 is the derived force deflection from the test instrumentation. As can be seen, the maximum dynamic deflection is approximately 29 inches. If the unloading side of the graph is examined, it can be seen that the crush at separation from the barrier is approximately 26 ½ inches. However, when the test report is examined, the maximum reported residual crush is found to be 21 ½ inches and the average residual crush is approximately 19 inches. This difference between crush at separation and reported residual crush has been observed in numerous frontal barrier impacts investigated by the authors. This indicates that the vehicle frontal structure continues to rebound after separation from the barrier. Since the vehicle structure rebounds after separation, neither the accelerometers nor the load cells will provide any measurement of the entire restitution of the structure. In order to use instrumentation to capture the structural restitution, a direct measurement method such as high speed film analysis, LDT's or other technique must be employed.



Figure 10. Force versus deflection – 1988 Toyota Camry.

PULSE MODELING

The expense and complication of full scale collision testing with automobiles often precludes its widespread use in the analysis of crash dynamics. Rather, the ability to readily control confounding variables leads the analyst to pursue sled testing or mathematical modeling. In order to perform either, it is necessary to input the crash test acceleration pulse. Additionally, it may be necessary to scale a known collision pulse to a different collision severity. The desire to duplicate a collision pulse, scale the collision pulse as well as program the collision pulse into a computer controlled sled leads to the selection of a closed form relationship such as a trigonometric or other function. In order to investigate the efficacy of various collision pulses, it is desirable to derive the necessary relationships in order to fit these analytical models to a collision pulse.

PULSE MODELING DERIVATIONS

When performing an accident reconstruction, numerous parameters are generally determined. These

parameters usually include the velocity profile and the amount of deformation to the vehicle under study. Therefore, it is desirable to create a model of the collision acceleration pulse from these known parameters. In order to develop a wide range in analytical relationships, the following functions were chosen to fit to an acceleration pulse between two objects. These functions include Sine, Haversine (\sin^2), triangular, and square wave. Figure 11 shows a graphical representation of the four chosen collision pulses. These functions are developed using the impact velocity, the change in velocity, and the mutual crush to the vehicles.

For the analysis the following nomenclature will be used:

a = acceleration
t = time
s = displacement

P = peak acceleration
T = duration of impact
 V_1 = initial velocity of vehicle 1
 V_2 = initial velocity of vehicle 2
 ΔV_1 = change in velocity of vehicle 1
 ΔV_2 = change in velocity of vehicle 2
T = Collision Pulse Time duration

As earlier described, the following input set was chosen because these are parameters usually determined in any accident reconstruction:

- V_{O1} = Impact Velocity of Vehicle 1
- V_{O2} = Impact Velocity of Vehicle 2
- ΔV_1 = Velocity Change of Vehicle 1
- ΔV_2 = Velocity Change of Vehicle 2
- Mutual crush = Total Crush to Both Vehicles

Outputs from the model will include the acceleration, velocity, and displacement time histories. Additionally, peak acceleration, average acceleration, and impact duration are also output from the models.

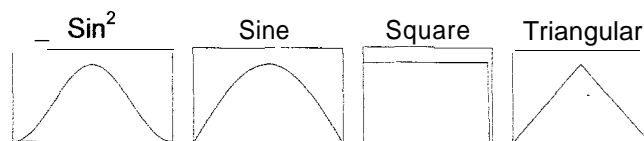


Figure 11. Graphical Representation of Pulses Used.

The Haversine pulse which is widely used for sled test input is used as an example of the model development. This pulse has been widely used to represent frontal barrier pulses and has been identified in previous research as being a good representation of a frontal barrier collision pulse [Breed, 1991]. The second model, the half period Sine pulse has also been previously identified in collision pulse modeling as a standard pulse to represent a frontal barrier impact [Breed, 1991]. The third collision pulse is the square wave which represents the collision as a constant acceleration. The fourth chosen collision model is the triangular pulse shape. This pulse shape has also been previously identified as a useful collision pulse model

[Brach,1991]. The development of the sine, triangular, and square wave collision pulse models are presented in the Appendix.

Model 1: Haversine (Sin²).

The acceleration is written as follows.

$$a = P \sin^2\left(\frac{\pi t}{T}\right) \quad \text{Eq. i}$$

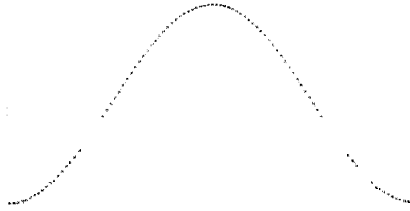


Figure 12. Graphical Representation: Sin*.

Integrating acceleration with respect to time yields velocity.

$$V = \frac{P}{4\pi} \left[2\pi t - T \cdot \sin\left(\frac{2\pi t}{T}\right) \right] + C_1 \quad \text{Eq. ii}$$

The integration constant C₁ can be determined through the knowledge that at t = 0, V = V_o. This yields C₁ = V_o.

Substituting C₁ into Equation ii yields

$$V = \frac{P}{4\pi} \left[2\pi t - T \cdot \sin\left(\frac{2\pi t}{T}\right) \right] + V_o \quad \text{Eq. iii}$$

At t = T, V = V_o + ΔV. Substituting into Equation iii yields peak acceleration.

$$P = \frac{2 \cdot \Delta V}{T} \quad \text{Eq. iv}$$

Integrating Equation iii yields displacement

$$s = \frac{T^2 \cdot P \cdot \cos\left(\frac{2\pi t}{T}\right) + 2\pi^2 \cdot t(Pt + 4V_o)}{8\pi^2} + C_2 \quad \text{Eq. v}$$

At t = 0, s = 0. Solving for C₂ yields

$$C_2 = \frac{-T^2 \cdot P}{8\pi^2} \quad \text{Eq. vi}$$

Substituting C₂ into Equation v yields the displacement as a function of time

$$S = \frac{T^2 \cdot P}{8\pi^2} \left[\cos\left(\frac{2\pi t}{T}\right) - 1 \right] + \frac{t}{4}(Pt + 4V_o) \quad \text{Eq. vii}$$

The final parameter to be determined is the duration of contact. At t₁ = t₂ = T, mutual crush = absolute value of s₁ - s₂. Solving Equation vii for impact duration results in the following determination of duration.

$$T = \frac{\text{mutual crush}}{\text{abs} \left[\frac{1}{2}(\Delta V_1 - \Delta V_2) + (V_{o1} - V_{o2}) \right]} \quad \text{Eq. viii}$$

MODEL APPLICATIONS

As can be seen in the Haversine derivation (along with those presented in the Appendix), analytical models can be applied to collision pulses. In fact, numerous other relationships can also be derived in the same fashion. In order to apply this data, first, an acceleration pulse is examined and the acceleration models are overlaid and examined with respect to the test data. Next, the best model is chosen and optimized to match the accelerometer output. As can be seen in the derivations, these relationships are developed to account for the complete acceleration pulse from contact through separation. In order to examine the ability of these curves to adequately model a simple collision pulse, a series of frontal barrier crash tests are examined. For this analysis, Vehicle 2 will be the barrier and Vehicle 1 will be the vehicle under study. Therefore, the only required inputs are the vehicle impact speed, AV and the vehicle crush. While the impact speed and AV may be determined through an examination of crash test data, the crush is a more difficult parameter to determine. It is important to remember that the developed collision pulse models are derived through separation. As a first modeling approximation, the average static (residual) crush can be input into the model. Figure 13 shows an acceleration pulse from a frontal barrier impact of a Dodge Neon along with the four collision pulse models. As can be seen, since the static crush occurs after complete structural restitution, and the derived equations only model through separation, the predicted acceleration pulses are significantly too short in duration.

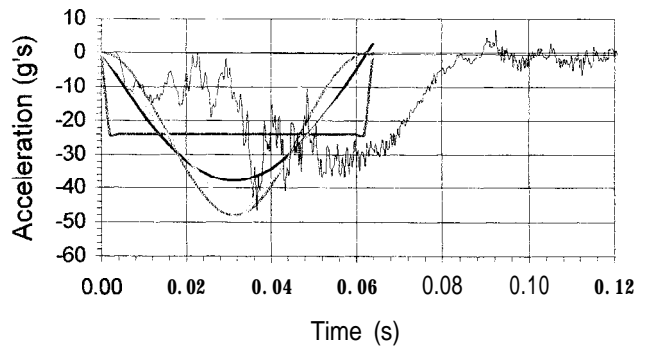


Figure 13. Use of Average Static Crush as input into pulse model - Dodge Neon

In order to examine the possibility that the endpoints of the static crush measurements are causing problems in the modeling exercise, the maximum static crush is then input into the model and the fit to the test curves is examined in Figure 14. As can be seen, the calculated collision duration is still significantly low due to insufficient crush being input in order to fit the models to the test data.

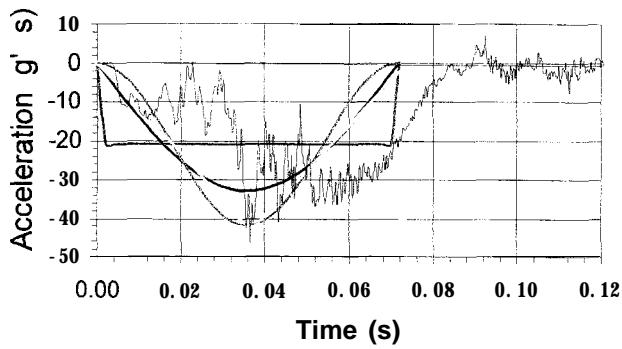


Figure 14. Use of Maximum Static Crush as input into pulse model - Dodge Neon

There exists several possibilities for additional methods to fit the derived models to actual collision test data. For instance, there may be a desire to only model the portion of the acceleration pulse up to zero velocity. Since the significant motions have already occurred, it is worth investigating whether the derived models appear to adequately model the motions to zero velocity, prior to rebound. Dynamic crush is input into the models and shown in Figure 15; the derived models fail to match the pulse shape; the inflection points and shape parameters from the analytical models fail to match the details seen in the acceleration pulse as recorded by instrumentation.

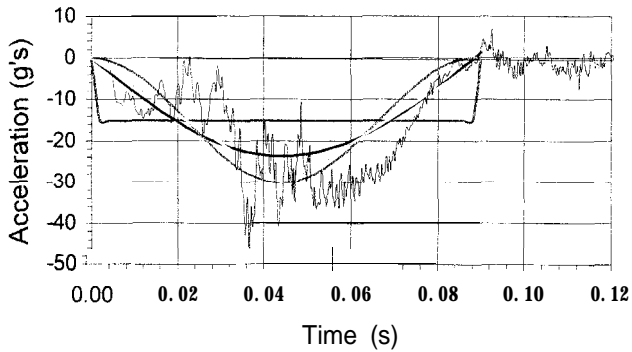


Figure 15. Use of Dynamic Crush and zero restitution as input into pulse model – Dodge Neon.

The examination of Figures 13-15, indicates the collision duration is consistently low or the shapes are poor representations of the crash pulses. That is due to the fact that one of the primary input data is the mutual crush to the vehicles being modeled. When modeling frontal rigid barrier collisions, this input crush is typically the residual crush to the vehicle under study. However, when examining the equations, one finds that the crush being input into the models is the crush at separation. As has been consistently seen, the static residual crush and the maximum residual crush for this vehicle both consistently underestimate collision duration. By examination of the equations, it is clear that the desired crush to be input is the crush at separation with the barrier. For this analysis, the assumption that this is the static residual crush results in incorrect modeling. As seen in Figure 10 for the Toyota, the Dodge Neon crush

at separation is also significantly greater than the measured residual crush. This phenomenon is seen frequently in collision test data. This slow to rebound structure continues with structural rebound even after separation with the barrier. Therefore, modeling the collision phase with the static residual crush, will result in consistently low collision duration.

Figures 16, 17, and 18 show the acceleration, velocity, and displacement time histories for all models fit to the test data using the crush at separation as the input criteria. Significantly better correlation is observed.

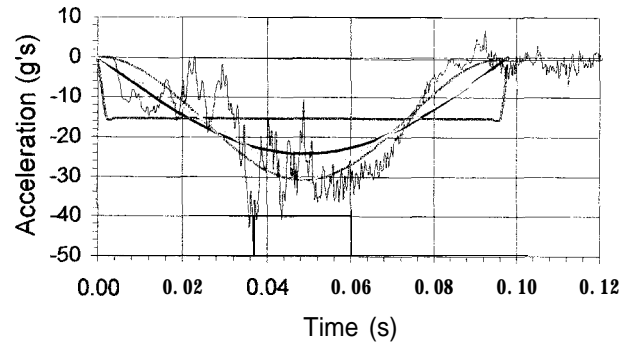


Figure 16. Use of Crush at Separation as input into pulse model – Acceleration Versus Time.

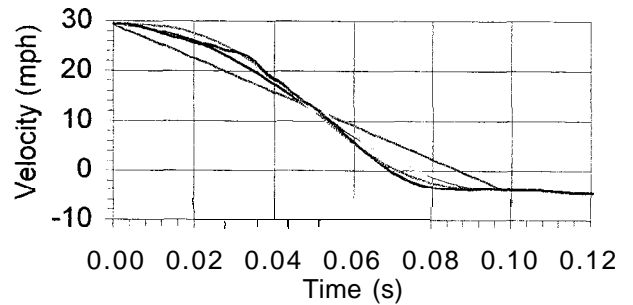


Figure 17. Use of Crush at Separation as input into pulse model – Velocity Versus Time.

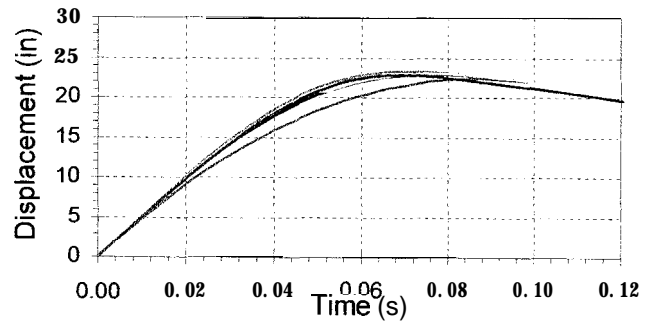


Figure 18. Use of Crush at Separation as input into pulse model – Displacement Versus Time.

The crush at separation is easily read from the force deflection chart as seen in Figure 19.

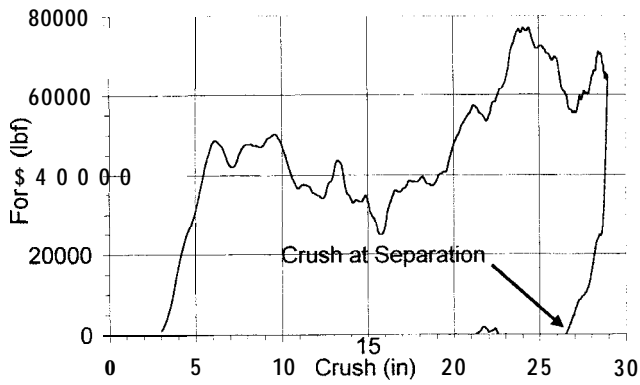


Figure 19. Force versus deflection.

VELOCITY SENSITIVITY

The concept of a distinctive pulse shape for a vehicle at all collision test speeds is attractive. This would allow the pulse shape to be determined based on a staged collision test at FMVSS or NCAP test velocity and then allow the scaling of that collision pulse to a velocity that corresponds with the reconstruction of a field accident. While it is not reasonable to generalize to all vehicles, this concept of a single pulse shape was investigated for two of the vehicles under study.

Consider the 1979 Ford E Series van. This vehicle was tested in a frontal barrier collision mode at test speeds of 15 and 30 mph. Upon examination and analysis of the acceleration-time history, it is found that a Sine model provides an adequate representation for both collision speeds, Figures 20-23.

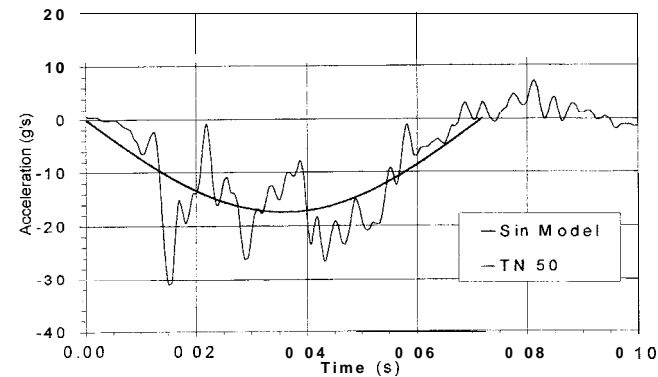


Figure 20. Acceleration Versus Time for Ford EI50 at 15.3 mph. Sine fit.

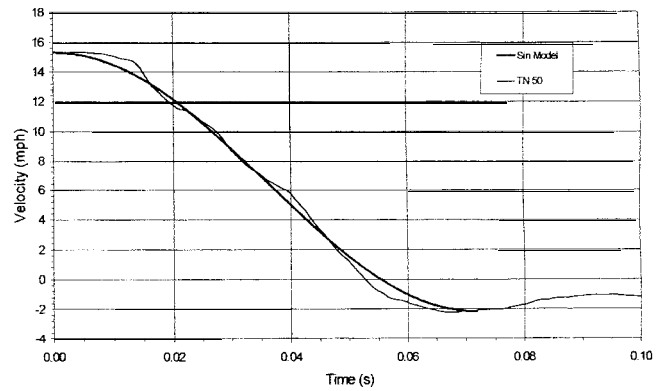


Figure 21. Velocity Versus Time for Ford EI50 at 15.3 mph. Sine fit.

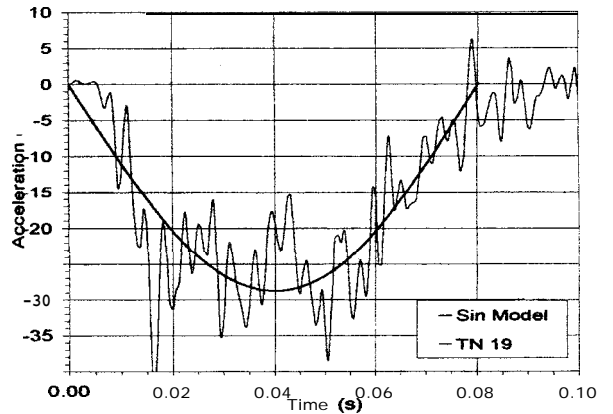


Figure 22. Acceleration Versus Time for Ford EI50 at 30.0 mph. Sine fit.

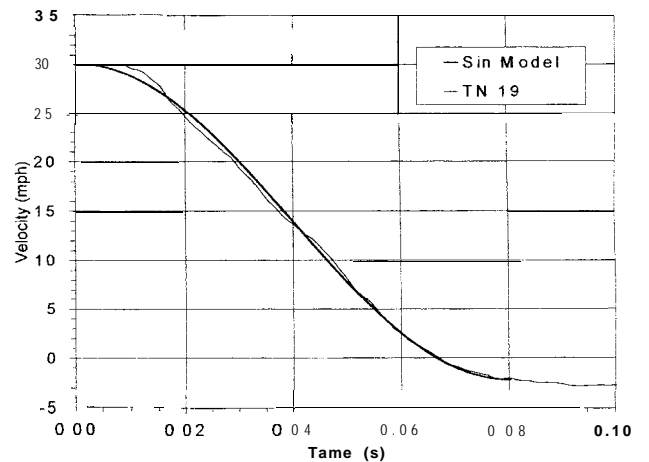


Figure 23. Velocity Versus Time for Ford EI50 at 30.0 mph. Sine fit.

The second analysis was performed with a series of crash tests of 1997 Hyundai Excels at 25, 30 and 35 mph. Once again, it can be seen that the sinusoidal model fits all of the collision tests speeds, Figures 24-27.

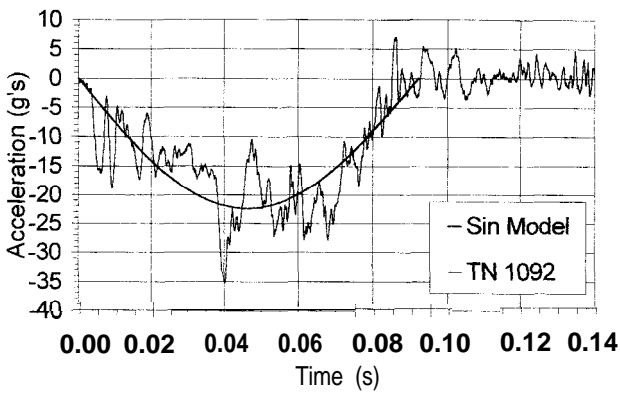


Figure 24. Acceleration Versus Time for Hyundai Excel at 24.7 mph. Sine fit.

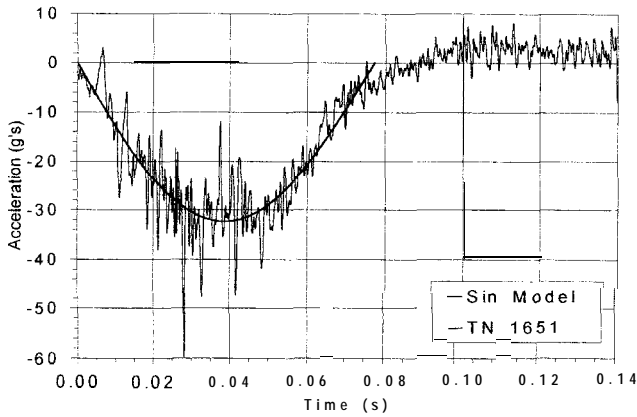


Figure 25. Acceleration Versus Time for Hyundai Excel at 29.6 mph. Sine fit.

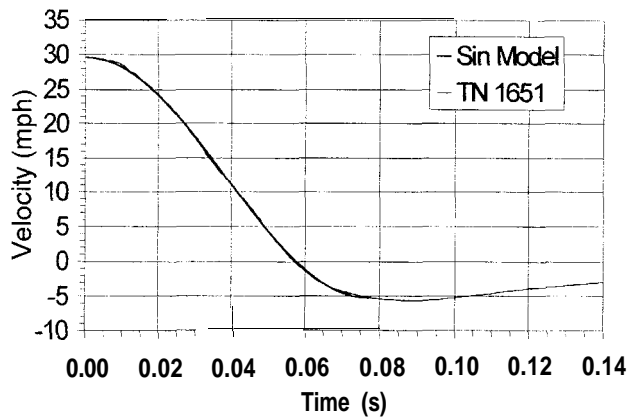


Figure 26. Velocity Versus Time for Hyundai Excel at 29.6 mph. Sine fit.

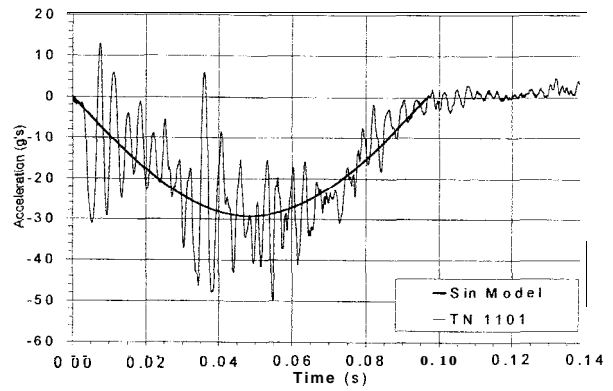


Figure 27. Acceleration Versus Time for Hyundai Excel at 35 mph. Sine fit.

MODELING DIFFERENT COLLISION MODES

To compare the usefulness of the presented equations to the modeling of offset frontal crashes, consider a Honda Accord full engagement frontal barrier NCAP crash. Figures 28 and 29 show the acceleration and velocity time history output from this test. Additionally, the Sine model curve fit is overlaid onto the test data.

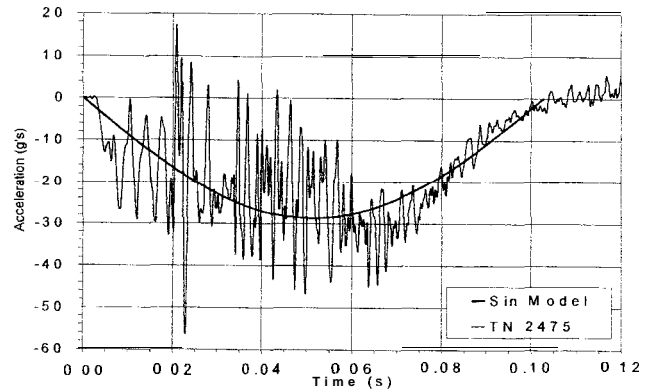


Figure 28. Acceleration Versus Time for Honda Accord Full Frontal Impact at 35 mph. Sine fit.

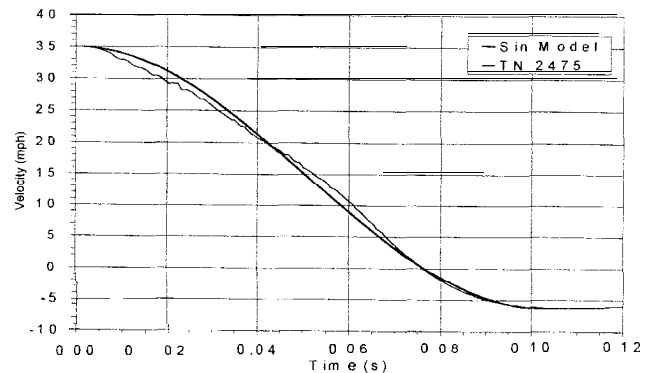


Figure 29. Velocity Versus Time for Honda Accord Full Frontal Impact at 35 mph. Sine fit.

While a Sine model serves as a useful model for the full engagement frontal test, a different pulse shape is seen for the offset frontal barrier test of the same vehicle. Figures 30 and 31 show the acceleration and velocity time histories from the offset frontal barrier test. Examination of these curves indicates that a triangular pulse more closely matches the instrumentation output

for this test data. These curves indicate pulse shape differences between the full frontal barrier test and the offset barrier collision test data for this vehicle.

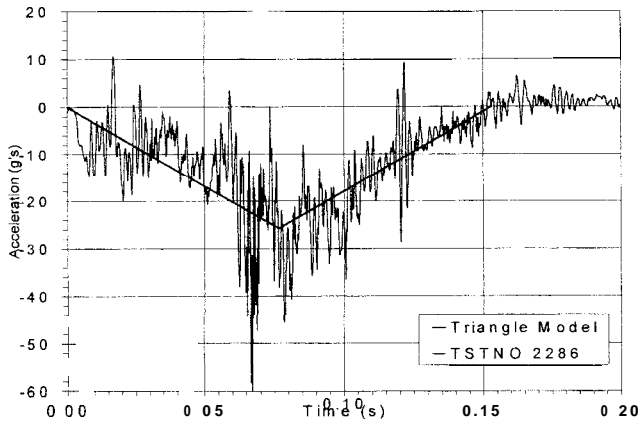


Figure 30. Acceleration Versus Time for Honda Accord 40% Offset Impact at 40 mph. Triangular fit.

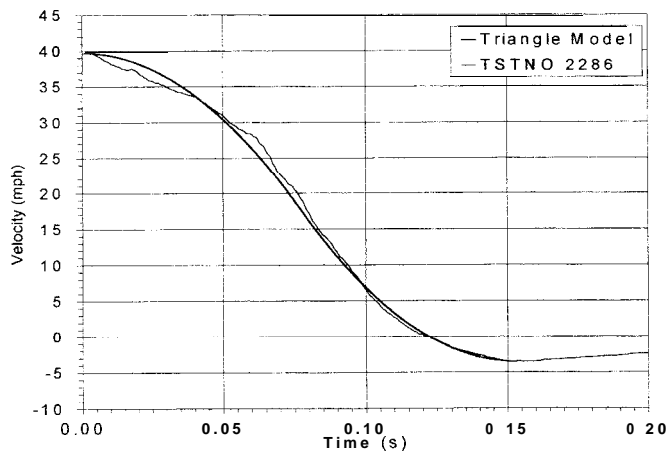


Figure 31. Velocity Versus Time for Honda Accord 40% Offset Impact at 40 mph. Triangular fit.

CONCLUSION

- Vehicle structural response is dependant on many characteristics which include vehicle and impact mode specific parameters. Care must be exercised when applying the data in this present research to a specific vehicle.
- The analysis of accelerometer data including sensor mounting location, repeatability, and the accuracy of load cell data has been explored.
- Sensor mounting location is important to consider when analyzing crash test data.
- Vehicle frontal impact tests, for those examined show repeatability when analyzing the vehicle structural response.
- Barrier load cell data has been shown to over-represent the amount of absorbed energy in a

frontal barrier collision. This over-representation of absorbed energy merits further analysis.

- Four collision pulse models have been derived and presented in order to analytically represent the response of a vehicle undergoing an impact.
- Inputs to the collision pulse models must be carefully considered. Impact speed, ΔV , and crush data require careful analysis.
- For the vehicles studied, some vehicle structural rebound takes place after separation from the barrier. This phenomenon prevents the structural rebound from being directly measured by either load cell or accelerometer instrumentation.
- Acceleration pulse models can be scaled to different impact velocities for the same vehicle but care must be used in application.
- Different crash modes with the same vehicle can exhibit different collision pulse shapes.

ACKNOWLEDGMENTS

The authors would like to acknowledge the work of Michael Stefani for his assistance in the analysis of the collision pulses.

ADDITIONAL SOURCES

Crash test instrumentation output may be downloaded directly from the NHTSA at <http://www.nhtsa.dot.gov/>.

Crash test reports, photographs, and data are available directly from the authors on CD or the National Crash Analysis Center, George Washington University Virginia Campus.

CONTACT

Questions and comments are welcome and should be addressed to the authors at:

KEVA Engineering
5636 LaCumbre Road
Somis, California 93066
www.kevaeng.com

REFERENCES

- Brach, R.M., Mechanical Impact Dynamics, John Wiley and Sons, Inc., New York, NY, 1991.
- Breed, D.S., Castelli, V., Sanders, W.T., A New Automobile Crash Sensor Tester, SAE Technical Paper 910655, Society of Automotive Engineers, Warrendale, PA, 1991.
- Kerkhoff, J.F., Husher, S.E., Varat, M.S., Busenga, A.M., Hamilton, K., An Investigation into Vehicle Frontal

impact Stiffness, BEV, and Repeated Testing for Reconstruction, SAE Technical Paper 930899, Society of Automotive Engineers, Warrendale, PA, 1993.

Machay, J.M., Gauthier, C.L., Results, Analysis and Conclusions of NHTSA's 35 mph Frontal Crash Repeatability Program, SAE Technical Paper #840201, Society of Automotive Engineers, Warrendale, PA, 1984.

Varat, MS., Husher, S.E., Kerkhoff, J.F., An Analysis of Trends of Vehicle Frontal Impact Stiffness, SAE Technical Paper 940914, Society of Automotive Engineers, Warrendale, PA, 1994.

APPENDIX – Sinusoidal, Square, and Triangular Pulse Derivations

Model 2: Sinusoidal Pulse.

The model evaluated is a Sine model to represent the acceleration pulse.

$$a = P \sin(\theta) \quad \text{Eq. 1}$$

$$\theta = \frac{\pi t}{T} \quad \text{Eq. 2}$$

where theta is chosen with boundary conditions that at $t = 0$, $a = 0$ and at $t = T$, $a = 0$.

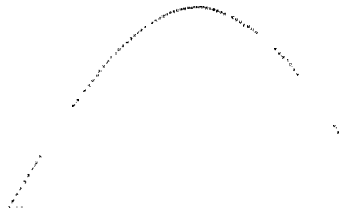


Figure A. Graphical Representation: Sine.

Integrating this acceleration yields the relationship for the velocity.

$$V = \frac{-T \cdot P \cdot \cos\left(\frac{\pi t}{T}\right)}{\pi} + C_1 \quad \text{Eq. 3}$$

The integration constant C_1 can be evaluated using the initial condition: at $t = 0$. $V = V_o$.

$$c_1 = \frac{T \cdot P}{\pi} + V_o \quad \text{Eq. 4}$$

Substituting C_1 into Equation 3

$$V = \frac{-T \cdot P \cdot \cos\left(\frac{\pi t}{T}\right)}{\pi} + \frac{T \cdot P}{\pi} + V_o \quad \text{Eq. 5}$$

The peak acceleration (P) can be found by solving Equation 5 knowing that at $t = T$, $V = V_o + \Delta V$.

$$P = \frac{\Delta V \cdot \pi}{2 \cdot T} \quad \text{Eq. 6}$$

The integration of velocity yields displacement.

$$S = \frac{-T^2 \cdot P \cdot \sin\left(\frac{\pi t}{T}\right)}{\pi^2} + t \left(V + \frac{T \cdot P}{\pi} \right) + C_2 \quad \text{Eq. 7}$$

C_2 is solved by knowing that at $t = 0$, $s = 0$, therefore

$$C_2 = 0 \quad \text{Eq. 8}$$

Substituting C_2 into Equation 7 gives displacement

$$S = \frac{-T^2 \cdot P \cdot \sin\left(\frac{\pi t}{T}\right)}{\pi^2} + t \left(V + \frac{T \cdot P}{\pi} \right) \quad \text{Eq. 9}$$

The acceleration, velocity, and displacement time histories all require the collision duration. The collision duration is determined through the following additional boundary condition: at $t_1 = t_2 = T$, mutual crush = $s_1 - s_2$. Substituting these conditions into the displacement time equation, yields the following equation for duration, T.

$$T = \frac{\text{mutual crush}}{\text{abs}\left[\left(V_{o_1} - V_{o_2} \right) + \left(\frac{\Delta V_1}{2} - \frac{\Delta V_2}{2} \right) \right]} \quad \text{Eq. 10}$$

Model 3: Square Pulse.

The third derived model is that of a simple square wave. For this relationship, peak and average accelerations are equal throughout the entire collision duration.

$$a = P \quad 0 \leq t \leq T \quad \text{Eq. 11}$$

Figure B. Graphical Representation; Square.

The integration of acceleration with respect to time yields velocity

$$v = Pt + C_1 \quad \text{Eq. 12}$$

At $t=0$, $V = V_0$. Solving for C_1

$$c_1 = V_0 \quad \text{Eq. 13}$$

Substituting C_1 into Equation 12

$$V = Pt + V_0 \quad \text{Eq. 14}$$

Solving for P at $t = T$, $V = V_0 + \Delta V$. The peak acceleration can now be determined. Note that the peak acceleration equals the average acceleration in this model.

$$P = \frac{\Delta V}{T} \quad \text{Eq. 15}$$

Integrate velocity to get displacement

$$S = \frac{1}{2}Pt^2 + V_0t + C_2 \quad \text{Eq. 16}$$

At $t = 0$, $S = 0$. C_2 can now be determined.

$$C_2 = 0 \quad \text{Eq. 17}$$

Substituting C_2 into Equation 16

$$S = \frac{1}{2}Pt^2 + V_0t \quad \text{Eq. 18}$$

At $t_1 = t_2 = T$, mutual crush = absolute value of $S_1 - S_2$. Solving for duration yields

$$T = \frac{\text{mutual crush}}{\text{abs}\left[\frac{1}{2}(\Delta V_1 - \Delta V_2) + (V_{o_1} - V_{o_2})\right]} \quad \text{Eq. 19}$$

Model 4: Triangular Pulse

The final derived model is that of a triangular wave.

$$\left[\begin{array}{l} a = \frac{2P}{T} \cdot t \quad 0 \leq t \leq \frac{T}{2} \\ a = -\frac{2P}{T} \cdot t + 2P \quad \frac{1}{2}T < t \leq T \end{array} \right] \quad \text{Eq. 20}$$

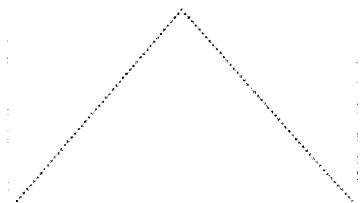


Figure C." Graph. Rerepresentation: Triangular.

The analysis of the triangular pulse is going to be performed in two parts. First, the time up to $t \leq \frac{1}{2}T$ is analyzed. For this time period, velocity is found by the integration of Equation 20 with respect to time

$$V = \frac{P}{T} \cdot t^2 + C_1 \quad \text{Eq. 21}$$

Using the known conditions, $V = V_0$ at $t = 0$, C_1 can be determined

$$c_1 = V_0 \quad \text{Eq. 22}$$

Substituting C_1 into Equation 21

$$V = \frac{P}{T}t^2 + V_0 \quad \text{For } t \leq \frac{1}{2}T \quad \text{Eq. 23}$$

Since the assigned triangular acceleration pulse is symmetrical about the midpoint, at time $t = \frac{1}{2}T$, the change in velocity will equal one half of the total change in velocity.

$$\text{At } t = \frac{T}{2} \quad V = \text{abs}(V_0 - \frac{1}{2}\Delta V) \quad \text{Eq. 24}$$

Assigning these boundary conditions allows the solution for the peak acceleration

$$P = \frac{2\Delta V}{T} \quad \text{Eq. 25}$$

Integrating Equation 23 with respect to time yields displacement

$$S = \frac{P}{3 \cdot T}t^3 + V_0t + C_2 \quad \text{Eq. 26}$$

At $t = 0$, $s = 0$. This allows the determination of C_2 .

$$C_2 = 0 \quad \text{Eq. 27}$$

Substituting C_2 into Equation 26

$$S = \frac{P}{3 \cdot T}t^3 + V_0t \quad \text{For } t \leq \frac{1}{2}T \quad \text{Eq. 28}$$

The preceding derivation must now be carried out for $t \geq \frac{1}{2}T$

Velocity is found by integrating Equation 28 with respect to time

$$V = \frac{-P}{T}t^2 + 2Pt + C_1 \quad \text{Eq. 30}$$

C_1 is arrived at by solving Equation 30 at time equal to one half of the duration.

$$V = \frac{P \cdot T}{4} + V_o \quad \text{Eq. 31}$$

Setting Equation 30 equal to Equation 31 allows for C_1 to be solved for.

$$C_1 = V_o - \frac{1}{2}P \cdot T \quad \text{Eq. 32}$$

Substituting C_1 into Equation 30 gives velocity

$$v = \frac{-P}{T}t^2 + 2Pt + V_o - \frac{1}{2}P \cdot T \quad \text{For } t \geq \frac{1}{2}T \quad \text{Eq. 33}$$

Integration of Equation 33 yields displacement

$$S = \frac{-P}{3T}t^3 + Pt^2 + V_o t - \frac{1}{2}P \cdot T \cdot t + C_2 \quad \text{Eq. 34}$$

By setting Equation 28 equal to Equation 34 at time equal to half the duration, C_2 can be determined.

$$C_2 = \frac{PT^2}{12} \quad \text{Eq. 35}$$

Substituting C_2 into Equation 34 results in:

$$S = \frac{-P}{3T}t^3 + Pt^2 + V_o t - \frac{1}{2}P \cdot T \cdot t + \frac{PT^2}{12} \quad \text{For } t \geq \frac{1}{2}T \quad \text{Eq. 36}$$

Combining the two derived relationships for displacement up to the collision mid point and then after the collision midpoint, the duration can be determined. At time $t = T$, the mutual crush = absolute value of $s_1 - s_2$. Algebraically solving for duration of impact yields the following:

$$T = \frac{\text{mutual crush}}{\text{abs} \left[\frac{2}{3}(\Delta V_1 - \Delta V_2) + (V_{o1} - V_{o2}) \right]} \quad \text{Eq. 37}$$

Vehicle Impact Response Analysis Through the Use Of Accelerometer Data

Michael S. Varat and Stein E. Husher
KEVA Engineering

Reprinted From: **Accident Reconstruction: Analysis, Simulation, and Visualization**
(SP-1491)